

# Polarization of $K$ -shell x-ray transitions of $\text{Ti}^{19+}$ and $\text{Ti}^{20+}$ excited by an electron beam

P. Beiersdorfer,<sup>1</sup> G. Brown,<sup>1</sup> S. Utter,<sup>1</sup> P. Neill,<sup>2</sup> K. J. Reed,<sup>1</sup> A. J. Smith,<sup>3</sup> and R. S. Thoe<sup>1</sup>

<sup>1</sup>*Department of Physics and Space Technology, Lawrence Livermore National Laboratory, Livermore, California 94551*

<sup>2</sup>*Department of Physics, University of Nevada, Reno, Nevada 89557*

<sup>3</sup>*Department of Physics, Morehouse College, Atlanta, Georgia 30314*

(Received 10 May 1999)

The x-ray spectrum of heliumlike  $\text{Ti}^{20+}$  excited by a monoenergetic electron beam was measured at an energy just above the electron-impact excitation threshold (4800 eV) with a pair of polarization-sensitive spectrometers. Values for the linear polarization were inferred for the  $1s2p\ ^1P_1 \rightarrow 1s^2\ ^1S_0$  resonance line, the  $1s2p\ ^3P_1 \rightarrow 1s^2\ ^1S_0$  intercombination line, the  $1s2p\ ^3P_2 \rightarrow 1s^2\ ^1S_0$  magnetic quadrupole line, and the  $1s2s\ ^3S_1 \rightarrow 1s^2\ ^1S_0$  forbidden line, as well as for the  $1s2s2p\ ^2P_{3/2} \rightarrow 1s^22s\ ^2S_{1/2}$  resonance line in  $\text{Ti}^{19+}$ . Relativistic distorted-wave calculations of the magnetic sublevel-specific electron-impact excitation cross sections are presented for comparison. Combined with earlier measurements of iron, the results confirm the predicted  $Z$  dependence of the polarization. [S1050-2947(99)07611-8]

PACS number(s): 34.80.Kw, 32.30.Rj, 32.70.Fw, 52.70.La

## I. INTRODUCTION

It has been shown that the polarization properties of x-ray lines can provide an important diagnostic tool for determining anisotropic electron distributions or even the presence and direction of beams in such high-temperature plasmas as the Sun [1,2] and, more recently, laser-produced plasmas [3,4]. X-ray polarization diagnostics are playing an increasingly important role in the understanding of ultrashort-pulse laser matter interactions, where calculations show that a substantial fraction of the laser energy is deposited in electron beams [5].

Despite its diagnostic utility, the use of x-ray polarization spectroscopy is still very much in its infancy. The reason is the complexity of the calculation and the lack of experimental verification of theoretical predictions in a controlled setting. Detailed calculations of the polarization properties of x-ray lines produced by directional electrons have been made mainly for  $K$ -shell transitions in one- or two-electron ions and have been limited to electron-impact excitation [1,6–9]. In a few cases, predictions of the linear polarization of x-ray lines excited by effects of resonant excitation by an electron beam [10], radiative recombination [11], and dielectronic recombination [12–15] have been made. Experimental tests of these calculations are almost nonexistent, since facilities capable of measuring the degree of polarization of an x-ray line from a highly charged ion excited by an electron beam in a controlled laboratory environment have only recently become available. Measurements are limited to the  $2 \rightarrow 1$   $K$ -shell transitions of heliumlike  $\text{Sc}^{19+}$  [16], heliumlike  $\text{Fe}^{24+}$  [17], and lithiumlike  $\text{Fe}^{23+}$  [18], and selected  $3 \rightarrow 2$   $L$ -shell transitions of lithiumlike  $\text{Fe}^{23+}$  and neonlike  $\text{Ba}^{46+}$  [19,20]. More experimental tests are needed to verify and stimulate theory and to advance the field of x-ray-based plasma polarization diagnostics.

In the following we present a measurement of the linear polarization of the  $K$ -shell transitions of  $\text{Ti}^{20+}$ . The measured lines comprise the  $1s2p\ ^1P_1 \rightarrow 1s^2\ ^1S_0$  resonance line, the  $1s2p\ ^3P_1 \rightarrow 1s^2\ ^1S_0$  intercombination line, the  $1s2p\ ^3P_2 \rightarrow 1s^2\ ^1S_0$  magnetic quadrupole line, and the

$1s2s\ ^3S_1 \rightarrow 1s^2\ ^1S_0$  forbidden line, labeled  $w$ ,  $y$ ,  $x$ , and  $z$ , respectively, in standard notation. The present measurement confirms and extends the earlier measurements of  $\text{Fe}^{24+}$  along the isoelectronic sequence. This is especially important for the intercombination line. Its polarization is strongly affected by relativistic effects in this range of atomic number where calculations rely on intermediate coupling. The present measurement also includes a determination of the  $1s2s2p\ ^2P_{3/2} \rightarrow 1s^22s\ ^2S_{1/2}$  transition in lithiumlike  $\text{Ti}^{19+}$ , labeled  $q$ , with a smaller uncertainty than the only previous measurement of lithiumlike  $\text{Fe}^{23+}$  [18].

## II. EXPERIMENTAL PROCEDURE

Like previous measurements of the linear polarization of x-ray lines, the present measurement of titanium was carried out using an electron beam ion trap. The source uses a monoenergetic electron beam ( $n_e \approx 10^{12} \text{ cm}^{-3}$ ) to excite ions confined in an electrostatic trap. This arrangement maximizes the linear polarization of the emitted x-ray lines and is optimal for testing theoretical predictions.

The  $K$ -shell x-ray lines of  $\text{Ti}^{20+}$  were analyzed in the plane perpendicular to the electron beam direction, i.e., at an observation angle  $\vartheta = 90^\circ$  relative to the  $z$  axis. At this observation angle, the polarization  $P$  is defined in the terms of the fractional difference between the intensity of light with electric field vector parallel to the beam direction,  $I_{\parallel}$ , and the intensity of light with electric field vector perpendicular,  $I_{\perp}$ ,

$$P = \frac{I_{\parallel} - I_{\perp}}{I_{\parallel} + I_{\perp}}. \quad (2.1)$$

The intensity of an x-ray line observed with a crystal spectrometer at  $90^\circ$  to the beam direction can be written as

$$I^{\text{obs}} = R_{\parallel} I_{\parallel} + R_{\perp} I_{\perp}. \quad (2.2)$$

Here,  $R_{\parallel}$  and  $R_{\perp}$  are the integrated crystal reflectivities for x rays polarized parallel and perpendicular to the electron beam directions, i.e., perpendicular and parallel to the plane

of dispersion, respectively. The relative reflectivity  $R = R_{\perp}/R_{\parallel}$  depends on the Bragg angle  $\theta$ . This fact is used to determine the polarization of a given x-ray line by employing the two-crystal measurement technique [18] to determine  $I_{\parallel}$  and  $I_{\perp}$ , and thus  $P$ . One spectrometer employs a Si(220) crystal observing a nearly pure polarization state, i.e., only  $I_{\parallel}$ , at a Bragg angle of  $\theta=43.1^{\circ}$ ; the second employs a Si(111) crystal observing a mixture of polarization states at a Bragg angle of  $\theta=24.7^{\circ}$ . The crystals behave like perfect crystals and the corresponding values of  $R$  are 0.029 and 0.579, respectively [21].

The two-crystal technique allows the determination of the polarization of any given line provided it can be referenced to a line with a known degree of polarization. The intensity ratio of two lines  $a$  and  $b$  observed with crystal 1 is given by

$$\frac{I^a}{I^b} \bigg|_1 = \frac{I_{\parallel}^a + R_1 I_{\perp}^a}{I_{\parallel}^b + R_1 I_{\perp}^b}. \quad (2.3)$$

Here, we assumed that  $R = R_{\perp}/R_{\parallel}$  is constant in the range of Bragg angles spanned by the two lines. Similarly, the ratio of the two lines observed with crystal 2 is

$$\frac{I^a}{I^b} \bigg|_2 = \frac{I_{\parallel}^a + R_2 I_{\perp}^a}{I_{\parallel}^b + R_2 I_{\perp}^b}. \quad (2.4)$$

TABLE I. Total cross section  $\sigma_{\text{total}}$  and fractional population density  $\sigma_m$  of magnetic sublevel  $m$  for electron-impact excitation from the  $1s^2\ ^1S_0$  ground state of heliumlike  $\text{Ti}^{20+}$  at an electron energy of 4800 eV. Numbers in brackets denote powers of ten.

Level	$\sigma_{\text{total}}$ ( $\text{cm}^2$ )	$\sigma_0$	$\sigma_{\pm 1}$	$\sigma_{\pm 2}$
$1s2p\ ^1P_1$	7.50[−22]	0.672	0.164	
$1s2p\ ^3P_0$	7.70[−23]	1.000		
$1s2p\ ^3P_1$	2.49[−22]	0.198	0.401	
$1s2p\ ^3P_2$	3.70[−22]	0.318	0.259	0.082
$1s2s\ ^1S_0$	2.61[−22]	1.000		
$1s2s\ ^3S_1$	1.23[−22]	0.333	0.333	

$$P_a = \frac{\frac{I^a}{I^b} \bigg|_1 \left( 1 + R_1 \frac{1 - P_b}{1 + P_b} \right) (R_2 + 1) - \frac{I^a}{I^b} \bigg|_2 \left( 1 + R_2 \frac{1 - P_b}{1 + P_b} \right) (R_1 + 1)}{\frac{I^a}{I^b} \bigg|_1 \left( 1 + R_1 \frac{1 - P_b}{1 + P_b} \right) (R_2 - 1) - \frac{I^a}{I^b} \bigg|_2 \left( 1 + R_2 \frac{1 - P_b}{1 + P_b} \right) (R_1 - 1)}. \quad (2.5)$$

All lines in the heliumlike system have varying degrees of polarization, and normalization to a reference standard with a known degree of polarization is not readily possible. However, we can make use of the fact that near threshold for electron-impact excitation the polarization of the forbidden line  $z$  is completely determined by that of line  $x$  because of cascade contributions from the  $1s2p\ ^3P_2$  level, as discussed in Ref. [17]. The expression for the polarization  $P_z$  of line  $z$  in terms of the polarization  $P_x$  of line  $x$  is [17]

$$P_z = + \frac{3kP_x}{3\sqrt{5/7} - P_x(\sqrt{5/7} + k)}. \quad (2.6)$$

Here, the factor  $k$  is given by

$$k = \sqrt{\frac{7}{20}} \frac{\beta_r \sigma_{\text{total}}(1s2p\ ^3P_2)}{\sigma_{\text{total}}(1s2s\ ^3S_1) + \sigma_{\text{total}}(1s2p\ ^3P_0) + \beta_r \sigma_{\text{total}}(1s2p\ ^3P_2)}, \quad (2.7)$$

where  $\beta_r = 0.2987$  is the branching ratio for  $^3P_2 \rightarrow ^3S_1$  decay [22] and  $\sigma_{\text{total}}$  denotes the total excitation cross section for the respective levels.

In Ref. [17] it was shown that the cross section for populating the  $^3P_2$  level remains constant relative to that for populating the  $^3P_0$  and  $^3S_1$  levels so that the ratio  $\sigma_{\text{total}}(^3P_2)/[\sigma_{\text{total}}(^3S_1) + \sigma_{\text{total}}(^3P_0) + \sigma_{\text{total}}(^3P_2)]$  remains constant at a value of about 0.645. This is borne out by the detailed values given in Table I for electron-impact excitation

of the magnetic sublevels of each  $n = 2$  level obtained from the relativistic distorted-wave computer code described in [7]. Therefore, the value of  $k$  depends only on  $\beta_r$ . We find  $k = 0.2106$ .

Alternatively, the  $1s2s2p\ ^2P_{1/2} \rightarrow 1s^22s\ ^2S_{1/2}$  line labeled  $r$  could be used for normalization. Because it emanates from an upper level with total angular momentum  $J = 1/2$ , its polarization is strictly 0 and represents a perfect reference line. The line is, however, too weak for reliable normalization.

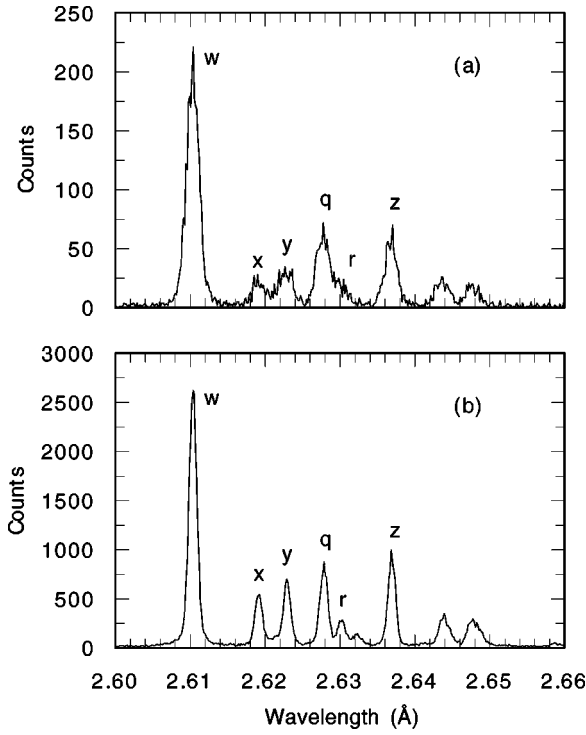


FIG. 1. Crystal-spectrometer spectra of lines  $w$ ,  $x$ ,  $y$ , and  $z$  in heliumlike  $\text{Ti}^{20+}$  and lines  $q$  and  $r$  in lithiumlike  $\text{Ti}^{19+}$  excited by a 4800-eV electron beam. (a) Spectrum obtained with a Si(220) crystal at a Bragg angle of  $43.1^\circ$ ; (b) spectrum obtained with a Si(111) crystal at a Bragg angle of  $24.7^\circ$ . Unlabeled features are inner-shell satellites from lower charge states.

### III. RESULTS

The spectra obtained simultaneously with the two spectrometers are shown in Fig. 1. The titanium ions were excited about 100 eV above the direct electron-impact excitation threshold ( $E_{\text{beam}} = 4800$  eV). The four transitions  $w$ ,  $x$ ,  $y$ , and  $z$  are clearly seen, as is lithiumlike line  $q$ . A few weaker, unlabeled lines populated by inner-shell excitation of lithiumlike  $\text{Ti}^{19+}$  and berylliumlike  $\text{Ti}^{18+}$  are also seen.

A von Hámos-type bent-crystal spectrometer [23] was used for the Si(220) measurement. A flat-crystal spectrometer [24] was used for the Si(111) measurement. The higher efficiency and resolving power of the bent-crystal spectrometer is evident from the spectra in Fig. 1, and the statistical accuracy is limited by the flat-crystal spectrum.

Comparing the two spectra, clear differences in the relative line intensities are found. The ratio of the  $\text{Ti}^{20+}$  triplet lines to the singlet line is considerably larger in the spectrum obtained at  $\theta = 24.7^\circ$ . This immediately indicates that the triplet lines have polarizations opposite to that of line  $w$ .

A listing of the measured intensities of the heliumlike and lithiumlike transitions is given in Table II. From these we determine  $P_w = +0.40^{+0.14}_{-0.12}$ ,  $P_x = -0.44^{+0.06}_{-0.06}$ ,  $P_y = -0.30^{+0.07}_{-0.07}$ ,  $P_z = -0.093^{+0.014}_{-0.013}$ , and  $P_q = +0.37^{+0.15}_{-0.10}$ . The error limits are given by a combination of the 68% statistical confidence limits in the measured intensity of each line and the uncertainties inherent in the crystal reflectivities.

Because the electrons have a small but finite thermal energy  $E_\perp$  in the plane perpendicular to their propagation, the measured polarization is somewhat less than it would be if

TABLE II. Intensities (adjusted for the spectrometer response function) and inferred linear polarization of the heliumlike lines  $w$ ,  $x$ ,  $y$ , and  $z$  and of the lithiumlike line  $q$  measured with Si(220) and Si(111) crystals. Theoretical polarization values are given for comparison.

Line	Ion	Si(220) (counts)	Si(111) (counts)	Predicted polarization	Measured polarization
$w$	$\text{Ti}^{20+}$	18976	1820	+0.608	$+0.43^{+0.14}_{-0.12}$
$x$	$\text{Ti}^{20+}$	3628	185	-0.519	$-0.48^{+0.06}_{-0.06}$
$y$	$\text{Ti}^{20+}$	4468	268	-0.339	$-0.33^{+0.07}_{-0.07}$
$z$	$\text{Ti}^{20+}$	6511	470	-0.106	$-0.101^{+0.014}_{-0.013}$
$q$	$\text{Ti}^{19+}$	5999	569	+0.341	$+0.40^{+0.15}_{-0.10}$

the electrons had no perpendicular velocity. The polarization  $P^0$  in the case of  $E_\perp = 0$  is related to the measured polarization [19,25] as

$$P^0 = \frac{2P}{2 - E_\perp(3 - P)/E_{\text{beam}}} \quad (3.1)$$

for the electric dipole transitions  $w$  and  $y$ . This expression also holds for the magnetic quadrupole transition  $x$ , as its set of orientation parameters resembles those of electric dipole transitions [17]. The expression for the magnetic dipole transition  $z$  is

$$P^0 = \frac{2P}{2 - E_\perp(3 + P)/E_{\text{beam}}}. \quad (3.2)$$

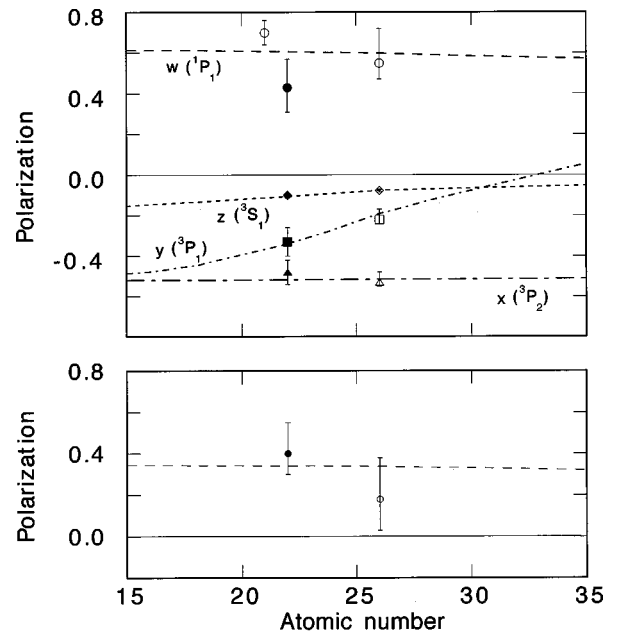


FIG. 2. Top: Predicted polarizations of the resonance line  $w$ , the intercombination lines  $x$  and  $y$ , and the forbidden line  $z$ . Nuclear effects, important for ions with a finite magnetic moment, are not taken into account. The values measured for  $\text{Ti}^{20+}$  are represented by solid symbols. Open symbols represent earlier measurements reported in Refs. [16] and [17]. Bottom: Predicted polarizations of the resonance line  $q$ . The value measured for  $\text{Ti}^{19+}$  is represented by a solid circle. The open circle represents the earlier measurement of  $\text{Fe}^{23+}$  reported in Ref. [18].

The amount of thermal energy depends on such parameters as the amount of beam compression or the tuning of the magnetic field at the cathode region of the electron gun. From the beam compression ratio, we estimated earlier a value of  $110 \pm 100$  eV [17]. Recent measurements have indicated values as high as 250 eV. Adjusting for a 250 eV thermal component provides the polarization values listed in Table II. The values are only marginally different from the unadjusted values, showing that precise knowledge of the thermal component is not important given the statistical uncertainties. Table II also lists the polarization values calculated from the theoretical cross-section data in Table I. The polarization calculated for line  $q$  is based on our calculation of the magnetic cross sections  $\sigma_{\pm 1/2} = 1.815 \times 10^{-22} \text{ cm}^2$  and  $\sigma_{\pm 3/2} = 5.834 \times 10^{-23} \text{ cm}^2$ .

#### IV. DISCUSSION

In Fig. 2 we compare the results of the present measurement of the  $\text{Ti}^{20+}$  lines with those of different ions as well as with theoretical predictions of the line polarizations of different heliumlike ions from relativistic distorted-wave calculations [17]. The new results for titanium confirm the theoretical predictions. Combined with the earlier measurement

of iron [17], the present measurement confirms the predicted variation in the polarization of lines  $y$  and  $z$  as a function of atomic number. For line  $y$  this variation is the result of relativity that mixes the triplet and singlet levels. For line  $z$  the variation is caused by the change in the population dynamics entailed by changes in the radiative branching ratio of the  $1s2s\ ^3P_2$  level.

Figure 2 also provides a comparison with theory of the polarization measured for the lithiumlike line  $q$ . Combined with the earlier datum from Ref. [18] for iron, the new datum for titanium confirms the predictions that, in the range of  $Z$  shown, the polarization of the lithiumlike resonance line remains constant.

#### ACKNOWLEDGMENTS

This work was performed under the auspices of the U.S. Department of Energy by Lawrence Livermore National Laboratory under Contract No. W-7405-ENG-48 and was supported in part by the Office of Basic Energy Sciences, Division of Chemical Physics. Additional support from the Livermore Collaborations Program for Historically Black Colleges and Universities is gratefully acknowledged.

- 
- [1] E. Haug, *Sol. Phys.* **71**, 77 (1981).
  - [2] I. A. Zhitnik *et al.*, in *X-Ray Spectroscopy and Properties of Multiply Charged Ions*, Proceedings of the Lebedev Physics Institute Vol. 179, edited by I. E. Sobelman (Nova Science Publishers, Commack, NY, 1988), p. 51.
  - [3] J. C. Kieffer *et al.*, *Phys. Rev. Lett.* **68**, 480 (1992).
  - [4] J. C. Kieffer *et al.*, *Phys. Rev. E* **48**, 4648 (1993).
  - [5] J. Dunn *et al.*, in *Laser Interactions and Related Phenomena*, AIP Conf. Proc. No. 369, edited by S. Nakai and G. H. Miley (AIP Press, New York, 1996), p. 652; N. Hasegawa, H. Nakagawa, H. Yoneda, K. Ueda, and H. Takuma, *ibid.*, p. 660.
  - [6] M. K. Inal and J. Dubau, *J. Phys. B* **20**, 4221 (1987).
  - [7] H. L. Zhang, D. H. Sampson, and R. E. H. Clark, *Phys. Rev. A* **41**, 198 (1990).
  - [8] Y. Itikawa, R. Srivastava, and K. Sakimoto, *Phys. Rev. A* **44**, 7195 (1993).
  - [9] K. J. Reed and M. H. Chen, *Phys. Rev. A* **48**, 3644 (1993).
  - [10] M. K. Inal and J. Dubau, *Phys. Rev. A* **47**, 4794 (1993).
  - [11] J. H. Scofield, *Phys. Rev. A* **40**, 3054 (1989).
  - [12] M. K. Inal and J. Dubau, *J. Phys. B* **22**, 3329 (1989).
  - [13] A. S. Shlyaptseva, R. C. Mancini, P. Neill, and P. Beiersdorfer, *Rev. Sci. Instrum.* **68**, 1095 (1997).
  - [14] A. S. Shlyaptseva *et al.*, *Phys. Rev. A* **57**, 888 (1998).
  - [15] A. S. Shlyaptseva, R. C. Mancini, P. Neill, and P. Beiersdorfer, *J. Phys. B* **32**, 1041 (1999).
  - [16] J. R. Henderson *et al.*, *Phys. Rev. Lett.* **65**, 705 (1990).
  - [17] P. Beiersdorfer *et al.*, *Phys. Rev. A* **53**, 3974 (1996).
  - [18] P. Beiersdorfer *et al.*, *Rev. Sci. Instrum.* **68**, 1073 (1997).
  - [19] D. W. Savin, M.-F. Gu, and P. Beiersdorfer, in *Proceedings of the US-Japan Workshop and International Seminar on Plasma Polarization Spectroscopy, Kyoto, Japan, 1998*, NIFS-PROC-37, edited by T. Fujimoto and P. Beiersdorfer (National Institute for Fusion Science, Toki, Gifu, 1998), pp. 90–102.
  - [20] E. Takács *et al.*, *Phys. Rev. A* **54**, 1342 (1996).
  - [21] B. L. Henke, E. M. Gullikson, and J. C. Davis, *At. Data Nucl. Data Tables* **54**, 181 (1993).
  - [22] C. D. Lin, W. R. Johnson, and A. Dalgarno, *Phys. Rev. A* **15**, 154 (1977).
  - [23] P. Beiersdorfer *et al.*, *Rev. Sci. Instrum.* **61**, 2338 (1990).
  - [24] P. Beiersdorfer and B. J. Wargelin, *Rev. Sci. Instrum.* **65**, 13 (1994).
  - [25] M.-F. Gu, D. W. Savin, and P. Beiersdorfer (unpublished).